Life-Cycle Cost Assessment of Climate Change Adaptation Measures to Minimise Carbonation-Induced Corrosion Risks

Mark G. Stewart[1]
Professor and Australian Research Council Professorial Fellow
Director, Centre for Infrastructure Performance and Reliability
The University of Newcastle
New South Wales, 2308, Australia
phone: +61 2 49216027 email: mark.stewart@newcastle.edu.au

Jianxin Peng
Lecturer
School of Civil Engineering and Architecture
Changsha University of Science & Technology
Changsha, Hunan 410114, China.

Published in:
International Journal of Engineering Under Uncertainty: Hazards, Assessment and Mitigation
2010, Vol. 2, Nos. 1-2, pp. 35-46

ABSTRACT

The paper describes a reliability-based approach that predicts the probability of corrosion initiation and damage (severe cracking) for RC structures subjected to corrosion resulting from concrete carbonation when atmospheric CO_2 concentration and temperature increases with time over the next 100 years based on the latest IPCC report for climate change. Increasing design cover is a suggested climate change adaptation strategy. A life-cycle cost analysis is then conducted that considers costs associated with extra design cover and expected maintenance/repairs for typical RC structures and elements over the next 100 years considering several IPCC atmospheric CO_2 emission scenarios. If the proposed increases in design cover produce a minimum life-cycle cost then increasing design cover will be a cost-effective measure to mitigate the effects of carbonation-induced corrosion damage. It was found that life-cycle costs for the current situation ('do nothing' – use existing covers) are lower than life-cycle costs for proposed increases in design cover. This suggests that although enhanced greenhouse conditions will lead to increased carbonation-induced corrosion of RC structures it may not be cost-effective to increase design covers.

[1] Corresponding Author

INTRODUCTION

Global warming and climate change studies show that greenhouse gas emissions (atmospheric CO_2) may more than double this century, causing temperature rises of up to 4.0 ^oC. An increase in atmospheric CO_2 concentrations will increase carbonation depths, and an increase in temperature will increase diffusion coefficient and corrosion rates, and so the likelihood and extent of carbonation-induced corrosion is expected to increase. This increase in carbonation and corrosion rate may cause corrosion damage that will need to be repaired or shorten the service life of reinforced concrete (RC) structures or elements, such as building facade panels, floor slabs and beam, bridges, etc. On the other hand, increasing the design cover, improved concrete quality, surface coatings, realkalization and other adaptation strategies for new and existing RC structures may help offset the effects of global warming.

While much work has progressed on the time-dependent structural reliability of deteriorating structures (mostly chloride-induced corrosion and fatigue), less effort has been directed to the probabilistic modelling of carbonation-induced cover cracking and structural collapse for RC structures. This is understandable as current levels of atmospheric CO_2 of about 380 ppm will, in many cases, not cause significant carbonation–induced corrosion (Stewart and Rosowsky 1998). Sudret (2008) developed spatial reliability models to predict the likelihood and extent of corrosion damage induced by carbonation, but this work assumed a constant (time-invariant) CO_2 concentration. However, climate change and global warming studies predict that the level of atmospheric CO_2 may increase to over 1000 ppm by the year 2100. As a consequence of this, carbonation may become a more critical durability issue for concrete structures in urban environments. Moreover, Stewart et al (2002) found that the ambient CO_2 concentration attributable to a typical urban environment is approximately 5-10 % higher than CO_2 concentrations in a rural environment. The concentration of CO_2 in urban environments are influenced by combustion of fossil fuels from traffic, domestic heating, power generation, etc, and CO_2 concentrations are often higher closer to ground level. Carbonation depths were then calculated for RC structures assuming a climate change prediction of up to 450 ppm for service lives of up to 100 years (Stewart et al 2002). The probabilistic analysis showed that variability in carbonation depths can he high due to uncertainty and variability of environmental and material properties. A model that predicts the effect of climate change on carbonation has been developed by Yoon et al (2007), but this model tends to overestimate carbonation depths. Peng and Stewart (2008) used the latest CO_2 concentration data provided by the fourth assessment report of 2007 Intergovernmental Panel Climate Change (IPCC) and the Yoon carbonation model to predict the likelihood and extent of carbonation-induced cover cracking and safety loss to RC and prestressed concrete beams in flexure and shear.

When developing reliability-based durability design specifications the fib Model Code for Service Life Design (fib 2006) adopted a CO_2 concentration of approximately 500 ppm based on a linear increase of 1.5 ppm/yr over 100 years. However, this work only considered corrosion initiation as the limit state, and the Intergovernmental Panel on Climate Change (IPCC) predict CO_2 concentrations of up to 1000 ppm by 2100. The present paper describes a reliability-based approach that predicts the probabilities of corrosion initiation and corrosion damage (severe cracking) for RC structures subjected to corrosion resulting from concrete carbonation when the atmospheric CO_2 concentration and temperature increases with time over the next 100 years based on the latest Intergovernmental Panel on Climate Change (IPCC) report for climate change. The carbonation model developed by Yoon et al (2007) is modified to better characterise the effect of time-dependent growth of CO_2 concentration on carbonation depth. In the present paper, 'corrosion damage' refers to corrosion-induced cover cracking with crack width exceeding 1.0 mm. Increases in design cover to offset the effects of increasing CO_2 concentrations are suggested for sheltered and unsheltered outdoor exposures. A life-cycle cost analysis is then conducted that considers costs associated with extra design cover and expected maintenance/repairs for typical RC structures and elements over the next 100 years considering several IPCC atmospheric CO_2 emission scenarios. If the proposed increases in design cover produce a minimum life-cycle cost then increasing design cover will be a cost-effective climate change adaptation measure to mitigate the effects of carbonation-induced corrosion damage.

For a sustainable future a life cycle analysis needs to consider environmental impacts of infrastructure design, construction and maintenance. A useful metric for such purposes is embodied energy, for example, the embodied energy for in-situ concrete is approximately 0.7-1.1 GJ/t whereas for structural steel it is 23-35 GJ/t (Collings 2006). However, embodied energies are difficult to estimate for concrete maintenance, user delay costs, etc. Nonetheless, Collings (2006) concludes that the environmental burden of a bridge is approximately proportional to its cost. Hence, the present paper will focus on life-cycle costs as a metric for energy requirements when assessing which design or repair options lead to a more sustainable future.

SPATIAL AND TEMPORAL VARIABILITY OF CO_2 CONCENTRATION AND TEMPERATURE

It has been recognised for some time that CO_2 concentrations are subject to temporal and spatial variability. Since the Industrial Revolution, CO_2 concentration in the atmospheric layer has been steadily increasing so that the global atmospheric concentration of CO_2 in 2000 is approximately 365 ppm (Meehl et al. 2007). The 2007 Intergovernmental Panel on Climate Change (IPCC) reported future CO_2 concentrations for six emission scenarios (Meehl et al. 2007). The two emission scenarios considered herein are:

(i) A1FI – This scenario describes a globalised future world of rapid economic growth and the rapid introduction of new and more efficient technologies with an emphasis on fossil intensive energy consumption. This is the worst case emissions scenario.

(ii) B1 – This scenario describes a globalised future world similar to the A1 family but with a rapid change in economic structures toward a service and information economy with reductions in material intensity and the introduction of clean and resource-efficient technologies. This is the lowest emissions scenario.

Both these scenarios assume that there are no controls/regulations to mitigate CO_2 emissions. The annual CO_2 concentration growth-rate is 1.9 ppm per year since 2000, and so the 'best mitigation' scenario after 2010 would be that the CO_2 concentration is kept stable at 2010 levels (386 ppm) due to reduction and stabilisation of CO_2 emissions. The fourth Assessment IPCC Report 2007 (AR4) was used for CO_2 emission scenarios for the next century (Meehl et al. 2007) which provided information about mean CO_2 concentrations as well as confidence bounds of mean ± one standard deviation (σ). The confidence bounds take into account the predictive model inaccuracies and inherent variabilities of CO_2 emissions and predicting their effect on atmospheric CO_2 concentrations. The mean and confidence bounds for A1FI and B1 emission scenarios as well as the best mitigation scenario are shown in Figure 1.

The standard deviations are approximated as

$$\sigma_{upper}(t) = X_{upper}(t - 2000) \quad \sigma_{lower}(t) = X_{lower}(t - 2000) \quad 2001 \le t \le 2100 \tag{1}$$

where $\sigma_{upper}(t)$ and $\sigma_{lower}(t)$ are the upper and lower bound standard deviations, respectively, and t is the time from 2001 to 2100. For A1F1 emissions scenario, X_{upper} and X_{lower} are 2.34 and 0.96, respectively. For B1 emissions scenario, X_{upper} and X_{lower} are 0.78 and 0.39, respectively.

A number of studies have shown elevated CO_2 levels in urban environments due to combustion of fossil fuels from traffic, domestic heating, power generation, pollutions, etc. Stewart et al. (2002) recorded CO_2 concentrations of up to 575 ppm in Brno (Czech Republic) which were 5-10% higher than rural CO_2 concentrations, with CO_2 concentrations higher near street level, see Figure 2. George et al. (2007) found that CO_2 concentrations in an urban site (Baltimore) were on average 16% higher than a rural site, and increases of 21-31% were reported in the literature. Day et al. (2002) observed an average enhancement over the course of the day in CO_2 concentration near an urban centre (Phoenix) of 19 ppm. As most infrastructure is located in urban environments, then atmospheric CO_2 concentrations shown in Figure 1 will be increased by a factor k_{urban}. In this paper k_{urban} is assumed normally distributed with mean of 1.15 and Coefficient of Variation (COV) of 0.10 for emission scenarios A1FI and B1. The factor k_{urban} is not applied to the best mitigation scenario as this scenario defines the best possible CO_2 outcome which would include minimal elevated CO_2 levels in urban environments.

The IPCC report (Meehl et al. 2007) also predicts increases in average global temperature as a result of increased CO_2 concentrations; namely, mean increases of 4.0 ^oC and 1.8 ^oC, for A1FI and B1 emission scenarios by 2100, respectively. The increase in temperature over time is approximately linear, and the variability is normally distributed with COV=0.3.

PROBABILITY OF CORROSION INITIATION AND DAMAGE

Time to Corrosion Initiation

The time to corrosion initiation (carbonation) depends on many parameters: concrete quality, concrete cover, relative humidity, ambient carbon dioxide concentration and others. The impact of carbonation has been studied by many researchers and various mathematical models have been developed with the purpose of predicting carbonation depths (for review see e.g., Duracrete 1998, Stewart et al 2002). Corrosion initiates at the time (T_i) when carbonation reaches the surface of the reinforcing bar.

The carbonation depth model proposed by Yoon et al. (2007) considers a wide range of influencing parameters and so the carbonation depth (x_c in cm) is predicted from Yoon et al. (2007), but corrected to allow for modelling uncertainties and k_{urban} as

$$x_c(t) = \sqrt{\frac{2D_{CO_2}(t)}{a} ME_{CO_2}(t) k_{urban} C_{CO_2}(t) t} \left(\frac{t_o}{t-1999}\right)^{n_m} \qquad t \geq 2000 \tag{2}$$

$$D_{CO_2}(t) = D_1 (t-1999)^{-n_d} \qquad a = 0.75 C_e C_a O \alpha_H \frac{M_{CO_2}}{M_{C_aO}} \tag{3}$$

where $ME_{CO_2}(t)$ is the time-dependent model error for CO_2 concentration with mean equal to one and variability obtained from Eqn. (1); $C_{CO_2}(t)$ is the time-dependent mass concentration of ambient CO_2 (10^{-3}kg/m^3) obtained from Figure 1 using the conversion factor 1 ppm = 0.0019×10^{-3} kg/m^3; k_{urban} is a factor to account for increased CO_2 levels in urban environments; $D_{CO_2}(t)$ is CO_2 diffusion coefficient in concrete; D_1 is the mean CO_2 diffusion coefficient after one year equal to 0.65, 1.24 and 2.23 for water-cement ratio (w/c) of 0.45, 0.5 and 0.55 respectively; n_d is the mean age factor equal to 0.218, 0.235 and 0.240 for w/c of 0.45, 0.5 and 0.55 respectively; C_e is cement content (kg/m^3) equal to 411, 370, and 336 for w/c of 0.45, 0.5 and 0.55 respectively; C_aO = 0.60; α_H = 0.78, 0.82 and 0.84 for w/c of 0.45, 0.5 and 0.55 respectively; M_{CaO} = 56 g/mol and M_{CO_2} = 44 g/mol; t_o is the reference period (1 year) and n_m is the age factor for microclimatic conditions (n_m=0 for sheltered outdooor, n_m=0.12 for unsheltered outdoor). Yoon et al (2007) provided estimates of maximum (95th percentile) values for D_1 and n_d. The standard deviation for D_1 is approximately 0.15, and COV for n_d is approximately 0.12 for all w/c ratios. These statistics represent model error (or accuracy). Note that the diffusion coefficient is consistent with other studies and so is appropriate for 'good quality concrete' (Sanjuan and del Olmo 2001).

The effect of temperature on diffusion coefficient is modelled using the Arrhenius Law (e.g., Duracrete 2000, Yoon et al 2007), where the time-dependent change in diffusion coefficient when compared to a temperature of 20 ^oC is:

$$f_T(t) = e^{\frac{E}{R}\left(\frac{1}{293}-\frac{1}{273+T(t)}\right)} \tag{4}$$

where T(t) is the temperature at time t (^oC), E is the activation energy of the diffusion process (40 kJ/mol) and R is the gas constant (8.314×10^{-3} kJ/mol·K). As temperature will be increasing over time then $D_{CO_2}(t)$ is averaged over time and so T(t) is also averaged over time.

While Eqn. (2) was used by Yoon et al (2007) to predict carbonation depths for increases in CO_2 concentrations it needs to be recognised that Eqn. (2) is a point-it-time predictive model - i.e., the carbonation depth at time t assumes that $CO_2(t)$ is constant for all times up to time t. This will overestimate carbonation depth as CO_2 concentration will be gradually increasing with time up to the peak value $CO_2(t)$. Stewart et al (2002) considered this phenomenon and calculated carbonation depths due to enhanced greenhouse CO_2 conditions using the average CO_2 concentration over the time period, and not the peak value at time t. As such, Eqn. (2) can be re-written as:

$$x_c(t) \approx \sqrt{\frac{2f_T(t)D_{CO_2}(t)}{a}k_{urban}\int_{2000}^{t} ME_{CO_2}(t)C_{CO_2}(t)dt}\left(\frac{t_o}{t-1999}\right)^{n_m} \qquad t \ge 2000 \tag{5}$$

where

$$f_T(t) \approx e^{\frac{E}{R}\left(\frac{1}{293}-\frac{1}{273+T_{av}(t)}\right)} \quad \text{and} \quad T_{av}(t) = \frac{\sum_{i=2000}^{t} T(t)}{t-1999} \tag{6}$$

To be sure, Eqn. (5) is an approximation, and there is a need for an improved carbonation model that considers the time-dependent effect of CO_2 concentration and other parameters such as temperature or humidity.

Corrosion-Induced Cover Cracking

The carbonation-induced corrosion rate is variable and highly dependent on exposure conditions and atmospheric situations – see Peng and Stewart (2008) for a review of corrosion rates. In the present study, corrosion rate is assumed lognormally distributed with statistical parameters for a temperature of 20 ^oC given by Duracrete (1998), see Table 1. An increase in temperature will increase corrosion rate, and the model described by Duracrete (2000) is used:

$$i_{corr}(t) = i_{corr-20}\left[1 + K(T(t) - 20)\right] \tag{7}$$

where $i_{corr-20}$ is the corrosion rate at 20 ^oC given in Table 1, and K=0.025 if T(t)<20 ^oC and K=0.073 if T(t)>20 ^oC. Duracrete (2000) notes that Eqn. (7) is a close correlation to Arrhenius equation, at least for temperature below 20 ^oC, but may be conservative for T(t)>20 ^oC. A 2^oC temperature increase will increase the diffusion coefficient and corrosion rate by 12% and 15%, respectively.

Corrosion-induced cover cracking occurs on the concrete surface above and parallel to the rebars. The various stages of crack growth can be described in three stages:

(i) Corrosion initiation (T_i);
(ii) Crack initiation (T_{1st}, time to first cracking - hairline crack of 0.05 mm width), and;
(iii) Crack propagation (T_{ser}, time for crack to develop from crack initiation to a limit crack width, w).

Time to Crack Initiation

As there is a porous zone around the steel reinforcing bar the corrosion products must firstly fill this porous zone before the products start to induce internal pressure on the surrounding concrete. Therefore, not all corrosion products contribute to the expansive pressure on the concrete. This approach to crack initiation has been used by El Maaddawy and Souki (2007) and their model is used herein. The thickness of the porous zone (δ_0) is typically in the range of 10 - 20 μm and can be described using a normal distribution with mean equal to 15 μm and COV of 0.1. It should be noted, that the accuracy of the time to severe cracking is dominated by the accuracy of time to corrosion initiation (T_i) and the time since crack initiation to reach a limit crack width (t_{ser}), and so service life predictions are relatively insensitive to the crack initiation model (Stewart and Mullard 2007).

Time to Severe Cracking

The time to severe cracking referred to herein is the time when concrete cover cracking reaches a limit crack width of 1 mm. Mullard and Stewart (2009) have modelled rate of crack propagation which enables the time for a crack to develop from crack initiation to a limit crack width (T_{ser}). The time (after corrosion initiation) for cracking of the concrete surface to reach a crack width of w mm is:

$$T_{sp} = T_{1st} + T_{ser} = T_{1st} + k_R \frac{w - 0.05}{k_c ME_{rcrack} r_{crack}} \left(\frac{0.0114}{i_{corr}}\right) \qquad 0.25 \le k_R \le 1,\ k_c \ge 1.0,\ w \le 1.0\text{mm} \tag{8}$$

where

$$\psi_{cp} = \frac{C}{Df_t} \tag{9}$$

$$r_{crack} = 0.0008e^{-1.7\psi_{cp}} \qquad 0.1 \le \psi_{cp} \le 1.0 \tag{10}$$

$$k_R \approx 0.95\left[\exp\left(-\frac{0.3 i_{corr(exp)}}{i_{corr}}\right) - \frac{i_{corr(exp)}}{2500 i_{corr}} + 0.3\right] \qquad k_R \ge 0.25 \tag{11}$$

and where T_{1st} is the time to crack initiation, T_{ser} is the time since crack initiation to reach a limit crack width (years), i_{corr} is the corrosion current density (μA/cm^2) assumed constant with time, ψ_{cp} is the cover cracking parameter, r_{crack} is the rate of crack propagation in mm/hr, ME_{rcrack} is crack propagation model error, w is the crack width (mm), C is concrete cover in mm, D is reinforcing bar diameter in mm, f_t is the concrete tensile strength in MPa, k_R is a rate of loading correction factor where $i_{corr(exp)}$=100 μA/cm^2 is the accelerated corrosion rate used to derive r_{crack}, and k_c is the confinement factor that represents an increase in crack propagation due to the lack of concrete confinement around external reinforcing bars. In this study, corrosion rates are assumed to remain constant with time (time-invariant).

If the reinforcing bar is in an internal location then k_c=1, but for rebars located at edges and corners of RC structures then k_c is in the range of 1.2 to 1.4. Although the data is limited, there appears to be a trend where k_c increases as ψ_{cp} increases. A statistical analysis of model accuracy to account for variabilities between model prediction and experimental data is essential for stochastic or reliability analyses where statistics for model error are required. Hence, the statistics for model error for r_{crack} (ME_{rcrack}) are: mean(ME_{rcrack}) = 1.04 and COV(ME_{rcrack}) = 0.09. For more details of this improved cover cracking model see Mullard and Stewart (2009).

Time-Dependent Reliability Analysis

Corrosion will take place when the carbonation depth reaches the surface of the reinforcing bar, and so the cumulative probability of corrosion initiation at time t is

$$p_i(t) = \Pr\left[C - x_c(t) < 0\right] \tag{12}$$

where C is the concrete cover and $x_c(t)$ is the carbonation depth obtained from Eqn. (5).

Corrosion damage is defined as the time when concrete cover severely cracks. Therefore, the cumulative probability of corrosion damage at time t is

$$p_s(t) = \Pr\left[t > T_i + T_{sp}\right] \tag{13}$$

Monte-Carlo simulation is used as a computational method for the time-dependent reliability analysis. Note that the CO_2 concentration is fully correlated with time.

Spatial effects for geometric and physical parameters known to influence structural reliabilities are not considered for general corrosion as their inclusion will be less important as it is for chloride-induced pitting corrosion (e.g., Stewart 2004). However, inclusion of spatial variability of environment, dimensions and material properties is an area for further research. It has been shown by Peng and Stewart (2008) that enhanced greenhouse conditions have negligible effect on structural reliability for flexure and shear limit states.

LIFE-CYCLE COST ANALYSIS

If the benefits of each alternative are the same, then the life-cycle cost up to time T, LCC(T), may be represented as

$$LCC(T) = C_D + C_C + C_{QA} + C_{IN}(T) + \sum_{i=1}^{M} p_{fi}(T)C_{SFi} \tag{14}$$

where C_D is the design cost, C_C the construction cost (materials and labour), C_{QA} the expected cost of quality assurance, C_{IN} (T) the cost of inspections, M the number of independent failure limit states (e.g., flexure, shear, spalling), $p_{fi}(T)$ the cumulative probability of failure for each limit state (i.e., probability that failure will occur anytime up to time T), and C_{SFi} the failure cost (i.e., damages, cost of life, injury, user delay, etc.) associated with the occurrence of each limit state. Costs and benefits may occur at different times so in order to obtain consistent results it is necessary for all costs and benefits to be discounted to a present value. Discount rates are influenced by a number of economic, social and political factors and thus can be quite variable. For example, discount rates used by various government agencies are: Australia 7%, U.S. 2-3%, UK Department of Transport, Sweden 4% and Finland 6% (Val and Stewart 2003). Note that a high discount rate favours a short service life whereas a low discount rate encourages longer service lives.

Since carbonation-induced corrosion of reinforcing steel has negligible influence on structural reliability then corrosion damage (severe corrosion-induced cracking) is considered as the most influential mode of failure for the estimation of life-cycle costs. If it is assumed that corrosion damage is always detected when the structure is inspected then the life-cycle cost given by Eqn. (14) may then be re-expressed as

$$LCC(T) = C_D + C_C + C_{QA} + C_{IN}(T) + E_{SF}(T) \tag{15}$$

where $E_{SF}(T)$ is the expected cost of corrosion damage during service life T and C_D, C_C, C_{IN} and C_M are all present value costs. For RC structures the expected cost of corrosion damage can be estimated as (Val and Stewart 2003):

$$E_{SF}(T) = \sum_{i=1}^{T/\Delta t} \Delta P_{f,i} \frac{C_{SF}}{(1+r)^{i\Delta t}} \tag{16}$$

where Δt is the time between inspections, C_{SF} the cost associated with the occurrence of corrosion damage (i.e., repair/replacement, user losses, etc.), r the discount rate, and $\Delta P_{f,i}$ is the probability of a damage incident between the $(i\text{-}1)^{th}$ and i^{th} inspections. This probability can be calculated by the following recursive formula

$$\Delta P_{f,i} = \left\{P_f(i\Delta t) - P_f\left[(i-1)\Delta t\right]\right\} + \sum_{j=1}^{i-1} \Delta P_{f,j}\left\{P_f\left[(i-j)\Delta t\right] - P_f\left[(i-j-1)\Delta t\right]\right\} \tag{17}$$

where $P_f(t)$ is the cumulative distribution function for the time of first damage – see Eqn. (13). The number of damage incidents n depends on the maintenance strategy. The maintenance strategy assumes that (Stewart 2001):

- repair is carried out immediately after corrosion damage has been discovered;
- limit state exceedance (Eqn. (13)) results in entire RC surface being repaired;
- repair provides no improvement in durability performance of the repaired structure (i.e., it is repaired with the same cover and concrete quality as the original design specification);
- damage may re-occur during the remaining service life of the structure, i.e., multiple repairs may be needed. The maximum possible number of damage incidents is $n_{max} = T/\Delta t$.

RESULTS

The statistical parameters for the reliability and life-cycle cost analyses are shown in Table 2. The specified concrete compressive strength is 30 MPa and water-cement ratio is 0.5. A concrete design cover of 30-40 mm is typical for many building structures such as internal structural members and wall panels for building facades under non-marine environments in many countries including the U.S. and Australia (i.e., ACI318 2005, AS3600 2001).

Probability of Corrosion Initiation

Figure 3 shows the mean carbonation depth for various emission scenarios and exposures. As expected, an outdoor sheltered exposure has a higher carbonation depths than unsheltered exposures because CO_2 diffusion is hindered by rain. For the worst case scenario (A1FI) the carbonation depths are 45% higher than that for the best mitigation scenario. This shows that future emission scenarios induced by economic development and population growth affects concrete carbonation and thus the onset of corrosion of reinforcing bars. The COV of carbonation depth is approximately 0.11. Figure 4 shows the probability of corrosion initiation (p_i) for RC structures with 30 mm cover (C_{nom}) and 16 mm diameter reinforcement for (a) sheltered and (b) unsheltered exposures. As seen in Figure 4, probabilities of corrosion initiation increase as the CO_2 concentration increases. When w/c=0.45 and in an unsheltered exposure then probability of corrosion initiation is negligible irrespective of the emission scenario. If design cover is increased to 40 mm the probabilities of corrosion initiation reduces significantly to no more than 0.02.

Probability of Corrosion Damage

Figure 5 shows the probability of corrosion damage (p_s) for RC structures with 30 mm cover and 16 mm diameter reinforcement for (a) sheltered and (b) unsheltered exposures. For the first 20-30 years of service life the effect of carbonation is negligible. If w/c=0.45 and in an unsheltered exposure then probability of corrosion damage is negligible irrespective of the emission scenario. The probability of corrosion damage for the worst case scenario (A1FI) is up to 500% higher than that observed for the best mitigation scenario. This indicates the higher CO_2 concentration could lead to a significant likelihood and extent of corrosion damage that may need costly and disruptive repairs during the service life of many concrete structures. A larger bar diameter will result in a corresponding higher likelihood of corrosion damage.

Adaptation Strategy - Increase in Design Cover

Table 3 shows the cumulative probability of corrosion damage in the year 2100 for existing covers under all emission scenarios for Y16 rebars with a w/c of 0.5 and sheltered exposure. In this study, the probability of corrosion damage (p_s) for the best mitigation scenario is taken as the baseline case. Table 3 then shows proposed covers needed for A1FI and B1 emission scenarios so that their reduced probabilities of corrosion damage match the baseline case. Therefore, it is found that existing design cover of 50 mm or less would need to increase by approximately 6-11 mm and 4-8 mm under A1FI and B1 emission scenarios, respectively. However, if existing design cover exceeds 50 mm then the probability of corrosion damage reaches near zero so there is no need for increases in design cover. Identical increases in design cover are needed to ameliorate corrosion damage for Y27 reinforcement (see Table 4). If w/c ratio is reduced to w/c=0.45 then probability of corrosion damage becomes negligible ($<10^{-4}$) for the best scenario, so large increases in cover are needed for A1FI and A1B emission scenarios to reduce damage risks to similarly low values, see Table 5. However, these large increases in cover may not be practical as the intent of adaptation strategies is not to reduce damage risks to negligible values. If the intent of code designs is not to reduce damage risks to negligible values then no extra cover is likely to be warranted if w/c=0.45. Finally, Table 6 shows that damage risks are also negligible for unsheltered exposure, and so for the same reasons cited above, no extra cover may be deemed appropriate. Clearly, there are many combinations of design variables so the intent of the present paper is to propose a methodology for assessing the need to adaptation strategies, and not to assess every combination of design variable.

Life-Cycle Cost Analysis

A life-cycle cost analysis is used to compare the mean life-cycle costs for two adaptation options:
(i) 'do nothing' – no change to design cover, and
(ii) increase design cover as proposed in Table 3.

For both adaptation options construction and repair cost data are needed, and such cost data is country, site and structure specific and so it is difficult to make generalisations about these costs. In this paper cost data will be taken from several sources and expressed in 2009 U.S. dollars. As we are concerned about outdoor CO_2 exposure then the external RC structural elements of interest are mainly beams and columns (assuming that slabs are mostly indoor exposures). Corrosion damage is assumed to occur on one (exposed) face of the structural element. The baseline case for construction cost including forms, concrete, reinforcement and finishing is approximately \$1,400/m^3 and \$2,400/m^3 for RC beams (8 m span) and columns (400 mm × 400 mm), respectively (RSMeans 2007). For a typical 500 mm deep × 300 mm wide RC beam then C_C=\$210/m length, and C_C=\$384/m for a RC column. It is assumed that an increase in design cover would increase cost of forms, concrete, reinforcement and finishing by an amount proportional to the extra volume of concrete needed. Hence, costs of this durability design specification (or quality - C_{QA}) are then estimated as C_{QA}=1/500=0.002C_C per mm cover/m or C_{QA}=1/400=0.0025C_C per mm cover/m for RC beams and columns, respectively. For a 20 mm increase in cover then C_{QA}=0.04-0.05C_C which is very similar to the costs reported by Troive and Sundquist (1998). Hence, in the analysis to follow C_{QA}=0.00225C_C per mm increase in cover. For the 'do nothing' option C_{QA}=0.

The cost of repair or replacement and associated user losses, etc. (C_{SF}) are considerable and for some structures user losses are often much greater than direct repair, replacement and maintenance costs. Val and Stewart (2003) assumed that the cost of RC bridge deck replacement is double the construction cost, i.e., C_{SF} = 2C_C based on cost data for (i) removal (C_C) and (ii) replacement (C_C) costs. However, this is likely to over-estimate the repair costs for most corrosion damage. A patch repair is the most common technique to repair corrosion damage in RC structures (e.g., BRE 2003, Canisius and Waleed 2004). The repair technique involves the removal of damaged concrete and replacement with a suitable repair material. The estimated cost for concrete patch repair is \$440/m^2 (BRE 2003). User losses and other user disruption costs are site and structure specific, but for many RC structures such costs will be minimised if the RC element to be repaired is an external structural member such as walls, columns or facade panels. To allow for a minor user disruption cost the total failure cost is assumed as C_F=\$500/m^2 which is C_{SF}=0.5×500/210=1.19C_C and C_{SF}=0.4×500/384=0.52C_C for RC beams and columns, respectively. The life-cycle cost analysis will consider two values of C_{SF}: (i) C_{SF}=0.5C_C and (ii) C_{SF}=1.5C_C to represent variability of failure costs. It is assumed that design and inspection costs (C_D, C_{IN}) are similar for different design specifications and so are not needed for this comparative analysis. The discount rate is assumed at r=3% and inspection interval is Δt=2 years.

Mean life-cycle costs are calculated from Eqn. (15) for A1FI and B1 emission scenarios for a design life of T=100 years, for (i) existing covers of 20 mm, 30 mm, 40 mm and 50 mm, and (ii) extra cover as shown in Table 3. Figure 6 shows that in all cases that life-cycle costs are less for the current ('do nothing') situation when compared to the adaptation option where design cover is increased. This is not surprising as even with the worst emissions scenario (A1FI) and lowest cover (20 mm) the probability of corrosion damage after 100 years is only 0.1584 (see Table 3). Because the probabilities of corrosion damage are relatively low there is negligible chance of multiple repairs (n>1). Hence, most structures will require no repair of corrosion damage, and so increasing the initial construction cost by up to C_{QA}=0.025C_C (11 mm increase in cover) is not cost-effective. However, the increases in life-cycle costs caused by increases in design cover are in the range of 0.9% to 1.9% - these are small increases in life-cycle costs which suggests that the benefit of not providing extra cover is marginal.

The inspection interval has negligible effect on life-cycle costs. If the discount rate changes to 2% or 4% then life-cycle costs increase (r=2%) or reduce (r=4%) slightly but the percentage difference changes by less than 0.4%. If the cost of providing extra cover is reduced from $0.00225C_C$ per mm cover to $0.0015C_C$ per mm cover then life-cycle costs for increase in design cover are 0.0% to 1.0% higher than life-cycle costs for the current ('do nothing') option. The percentage difference between the current situation and adaptation option reduces slightly if the cost of repair/replacement increases to $C_{SF} = 2.0C_C$. These sensitivity analyses show that for all reasonable combinations of input variables that the trend of the results is unchanged; namely, life-cycle costs for the current ('do nothing') option are lower than life-cycle costs for proposed increases in design cover. This suggests that although enhanced greenhouse conditions will lead to increased carbonation-induced corrosion of RC structures, the probability of corrosion damage remains low and so it is not cost-effective to increase existing covers. As life-cycle costs reflect the energy burden of structures, it is also reasonable to suggest that increases in design cover will lead to increased embodied energy use over the life-cycle of most RC structures. Note that improved concrete quality, surface coatings, realkalization, etc. may prove to be more cost-effective and sustainable climate change adaptation strategies than increasing design cover.

The primary anthropogenic factor associated with climate change is CO_2 concentration and temperature, but other climatic variables such as humidity and rainfall are predicted to change. Uncertainty about these and other climatic variables is very large (as is their spatial variability), and this uncertainty increases when the effects of potential CO_2 mitigation measures are considered. The effect of humidity and other climatic variables on risks of corrosion damage is clearly an area for further research.

A study of this nature necessitates many assumptions as we are dealing with a long time span where the impact of political and socio-economic issues on greenhouse CO_2 emissions is unclear. Furthermore, the effects of climate change are spatial, as well as temporal, so climate adaptation strategies to reduce risks of infrastructure deterioration will be region or site-specific. The present paper provides a decision-support framework to help address these issues, and the results provided are indicative for the structural configurations considered herein. Clearly, further research is needed to better characterise the temporal and spatial impacts of climate change, and the cost-effectiveness of adaptation strategies.

CONCLUSIONS

Global warming and climate change studies show that greenhouse gas emissions (atmospheric CO_2) may more than double this century. The paper described a reliability-based approach that predicts the probabilities of corrosion initiation and corrosion damage (severe cracking) and the recommended increase in design cover to offset the effects of increasing CO_2 concentrations and associated increase in temperatures. A life-cycle costs analysis considered initial construction costs and the costs of providing extra design cover and expected maintenance/repairs for typical RC structures and elements over the next 100 years considering several IPCC atmospheric CO_2 emission scenarios. It was found that life-cycle costs for the current situation (use existing covers) are lower than life-cycle costs for proposed increases in design cover. This suggests that although enhanced greenhouse conditions will lead to increased carbonation-induced corrosion of RC structures it may not be cost-effective to increase design covers.

REFERENCES

ACI 318 (2005). Building code requirements for structural concrete. Detroit, Michigan.

AS3600 (2001). Concrete structures. Standard Association Australia, Homebush, New South Wales, Australia.

BRE (2003), *Residual Life Models for Concrete Repair - Assessment of the Concrete Repair Process*, Building Research Establishment, UK.

Canisius, T.D.G. and Waleed, N. (2004), Concrete Patch Repairs Under Propped and Unpropped Implementation, *Structures and Buildings*, 157(SB2):149-156.

Collings, D. (2006), An Environmental Comparison of Bridge Forms, *Proc of the Inst. of Civil Engineers – Bridge Engineering*, 159(BE4): 163-168.

Day, T.A., Gober, P., Xiaong, F.S. and Wentz, E. (2002), Temporal Patterns in Near Surface CO2 Concentrations over Contrasting Vegetation Types in the Pheonix Metropolitan Area, *Agriculture and Forest Meteorology*, 110: 229-245.

DuraCrete (1998), *Modelling of Degradation*, DuraCrete - Probabilistic Performance based Durability Design of Concrete Structures, EU - Brite EuRam III, Contract BRPR-CT95-0132, Project BE95-1347/R4-5, December 1998, 174 p.

DuraCrete (2000), *Statistical Quantification of the Variables in the Limit State Functions*, DuraCrete - Probabilistic Performance based Durability Design of Concrete Structures, EU - Brite EuRam III, Contract BRPR-CT95-0132, Project BE95-1347/R9, January 2000, 130 p.

El Maaddawy, T. and Soudki, K. (2007). A model for prediction of time from corrosion initiation to corrosion cracking. *Cement & Concrete Composite*, 29(3): 168-175.

fib (2006), *Model Code for Service Life Design*, fib, Bulletin 34, February 2006, Lausanne.

George, K., Ziska, L.H., Bunce, J.A. and Quebedeaux, B. (2007), Elevated Atmospheric CO2 Concentration and Temperature Across an Urban-Rural Transect, *Atmospheric Environment*, 41: 7654-7665.

Meehl, G.A., Stocker, T.F., Collins, W.D., Friedlingstein, P., Gaye, A.T., Gregory, J.M., Kitoh, A., Knutti, R., Murphy, J.M., Noda, A., Raper, S.C.B., Watterson, I.G., Weaver, A.J., and Zhao, Z.-C. (2007). *Global climate projections.* In: Climate Change 2007: The Physical Science Basis. Contribution of Working Group I to the Fourth Assessment Report of the Intergovernmental Panel on Climate Change. Cambridge University Press: 789-812.

Mirza, S. A. and MacGregor, J. G. (1979), Variations in dimensions of reinforced concrete members. *Journal of Structural Division, ASCE*, 105(ST4): 751-766.

Mirza S. A., Hatzinikolas, M. and MacGregor, J. G. (1979), Statistical descriptions of strength of concrete. *Journal of Structural Division, ASCE*, 105(ST6):1021-1037.

Mullard JA, Stewart MG (2009), *Corrosion-Induced Cover Cracking of RC Structures: New Experimental Data and Predictive Models*, Research Report No. 275.01.2009, Centre for Infrastructure Performance and Reliability, The University of Newcastle, NSW, Australia.

Peng, J. and Stewart, M.G. (2008), *Carbonation-Induced Corrosion Damage and Structural Safety for Concrete Under Enhanced Greenhouse Conditions*, Research Report No. 270.11.2008, Centre for Infrastructure Performance and Reliability, The University of Newcastle, NSW, Australia.

RSMeans (2007), *RSMeans Building Construction Cost Data*, 65th Annual Edition, RSMeans, Kingston, MA.

Sanjuan, M.A. and del Olmo, C. (2001), Carbonation Resistance of One Industrial Mortar Used as a Concrete Coating, *Building and Environment*, 36(8): 949-953.

Stewart, M.G. and Rosowsky, D.V. (1998), Structural Safety and Serviceability of Concrete Bridges Subject to Corrosion, *Journal of Infrastructure Systems*, ASCE, 4(4): 146-155.

Stewart, M.G. (2001), Spalling risks, durability and life-cycle costs for RC buildings. In: Proc Int Conf on Safety, Risk and Reliability – Trends in Engineering, IABSE: 537-542.

Stewart, M.G., Teply, B. and Kralova, H. (2002), The Effect of Temporal and Spatial Variability of Ambient Carbon Dioxide Concentrations on Carbonation of RC Structures, *9th International Conference on Durability of Building Materials and Components,* CSIRO, Paper 246 (CD-ROM).

Stewart, M.G. (2004). Spatial variability of pitting corrosion and its influence on structural fragility and reliability of RC beams in flexure. *Structural Safety*, 26(4): 453-470.

Stewart, M.G. and Mullard, J.A. (2007). Spatial time-dependent reliability analysis of corrosion damage and the timing of first repair for RC structures. *Engineering Structures*, 29(7): 1457-1464.

Stewart, M. G. (1995), Workmanship and its influence on probabilistic models of concrete compressive strength. *ACI Materials Journal*, 92(4): 361-372.

Sudret, B. (2008), Probabilistic models for the extent of damage in degrading reinforced concrete structures, *Reliability Engineering and System Safety*, 93(3): 10-422.

Troive, S. and Sundquist, H. (1998), Optimisation of design parameters for lowest life-cycle cost of concrete bridges. In: Dunaszegi L, editor. *Proc 5th Int Conf on Developments in Short and Medium Span Bridge Engineering'98*, Calgary, July 1998. Montreal, Quebec: The Canadian Society for Civil Engineering: 1101-1113.

Val, D.V. and Stewart, M.G. (2003), Life Cycle Cost Analysis of Reinforced Concrete Structures in Marine Environments, *Structural Safety,* 25(4): 343-362.

Yoon, I.S., Copuroglu, O. and Park, K.B. (2007). Effect of global climatic change on carbonation progress of concrete. *Atmospheric Environment*, 41: 7274-7285.

Exposure Class	Mean	Standard Deviation
Carbonation		
Dry	0	0
Wet- rarely dry (unsheltered)	0.345 $\mu A/cm^2$	0.259 $\mu A/cm^2$
Moderate humidity (sheltered)	0.172 $\mu A/cm^2$	0.086 $\mu A/cm^2$
Cyclic wet-dry (unsheltered)	0.431 $\mu A/cm^2$	0.259 $\mu A/cm^2$

Table 1. Carbonation Corrosion Rates for Various Exposures (Duracrete 1998), for 20 ^oC.

Parameters	Mean	COV	Distribution	Reference
f'_{cyl} cylinder strength	37.5 MPa	σ=6 MPa	Lognormal	Stewart (1995)
k_w ($f'_c = k_w f'_{cy1}$)	0.87	0.06	Normal	Stewart (1995)
ME_{CO_2}	1.0	Eqn. (1)	Normal[a]	-
D_1	-	σ=0.15	Normal	Yoon et al (2007)
n_d	-	0.12	Normal	Yoon et al (2007)
$ME(r_{crack})$	1.04	0.09	Normal	Mullard & Stewart (2009)
k_{urban}	1.15	0.10	Normal[b]	-
Cover	C_{nom} +1.6 mm	σ=11.1 mm	Normal[c]	Mirza & MacGregor (1979)
f_t	$0.53(f_c)^{0.5}$	0.13	Normal	Mirza et al (1979)
E_c	$4600(f_c)^{0.5}$	0.12	Normal	Mirza et al (1979)
δ_0	15 μm	0.1	Normal	-

a: censored at 380 ppm, b: truncated at 1.0, c: truncated at 10 mm (stirrup diameter)

Table 2. Statistical Parameters for Corrosion Parameters, Material Properties and Dimensions.

Existing Cover (mm)	p_s (w=1 mm, t =100 years)			Proposed Cover (mm)	
	A1FI	B1	Best Mitigation	A1FI	B1
20	0.1584	0.1084	0.0405	31	28
30	0.0483	0.0301	0.0102	38	36
40	0.0076	0.0042	0.0014	47	44
50	0.0005	0.0002	0.0001	56	54
60	0.0	0.0	0.0	60	60

Note: 0.0 denotes $p_s<1\times10^{-4}$

Table 3. Probabilities of Corrosion Damage (p_s) for Existing Covers and Proposed Design Covers for A1FI and B1 Emission Scenarios for Y16 Rebar with a w/c of 0.5 and Sheltered Exposure.

Existing Cover (mm)	p_s (w=1 mm, t =100 years)			Proposed Cover (mm)	
	A1FI	B1	Best Mitigation	A1FI	B1
20	0.1780	0.1212	0.0461	31	28
30	0.0561	0.0343	0.0112	38	36
40	0.0092	0.0049	0.0016	47	44
50	0.0007	0.0003	0.0001	56	55
60	0.0	0.0	0.0	60	60

Note: 0.0 denotes $p_s<1\times10^{-4}$

Table 4. Probabilities of Corrosion Damage (p_s) for Existing Covers and Proposed Design Covers for A1FI and B1 Emission Scenarios for Y27 Rebar with a w/c of 0.5 and Sheltered Exposure.

Existing Cover (mm)	p_s (w=1 mm, t =100 years)			Proposed Cover (mm)	
	A1FI	B1	Best Mitigation	A1FI	B1
20	0.0447	0.0182	0.0008	42	38
30	0.0116	0.0043	0.0002	46	44
40	0.0015	0.0006	0.0	50	46
50	0.0001	0.0	0.0	50	50
60	0.0	0.0	0.0	60	60

Note: 0.0 denotes $p_s<1\times10^{-4}$

Table 5. Probabilities of Corrosion Damage (p_s) for Existing Covers and Proposed Design Covers for A1FI and B1 Emission Scenarios for Y16 Rebar with a w/c of 0.45 and Sheltered Exposure.

Existing Cover (mm)	p_s (w=1 mm, t =100 years)			Proposed Cover (mm)	
	A1FI	B1	Best Mitigation	A1FI	B1
20	0.0095	0.0016	0.0	46	40
30	0.0023	0.0004	0.0	46	40
40	0.0003	0.0	0.0	46	40
50	0.0	0.0	0.0	50	50
60	0.0	0.0	0.0	60	60

Note: 0.0 denotes $p_s<1\times10^{-4}$

Table 6. Probabilities of Corrosion Damage (p_s) for Existing Covers and Proposed Design Covers for A1FI and B1 Emission Scenarios for Y16 Rebar with a w/c of 0.5 and Unsheltered Exposure.

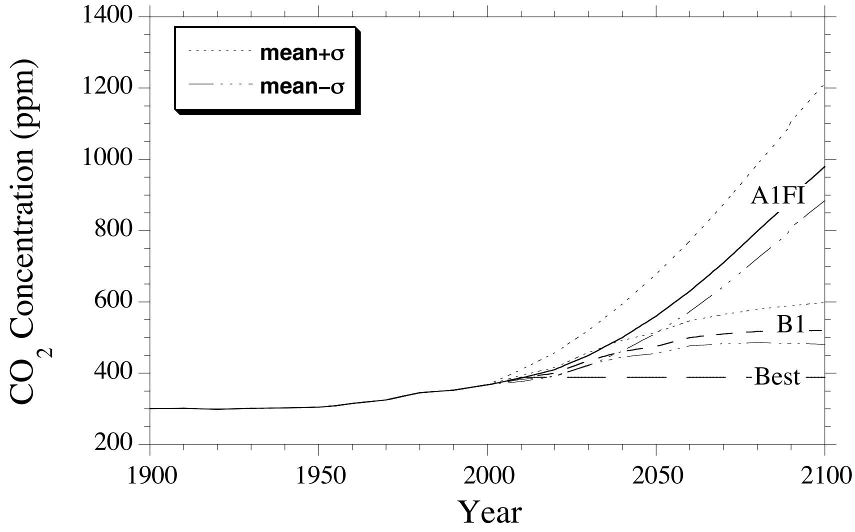

Figure 1. Time-dependent Change of Atmospheric CO_2 Concentration (Peng and Stewart 2008).

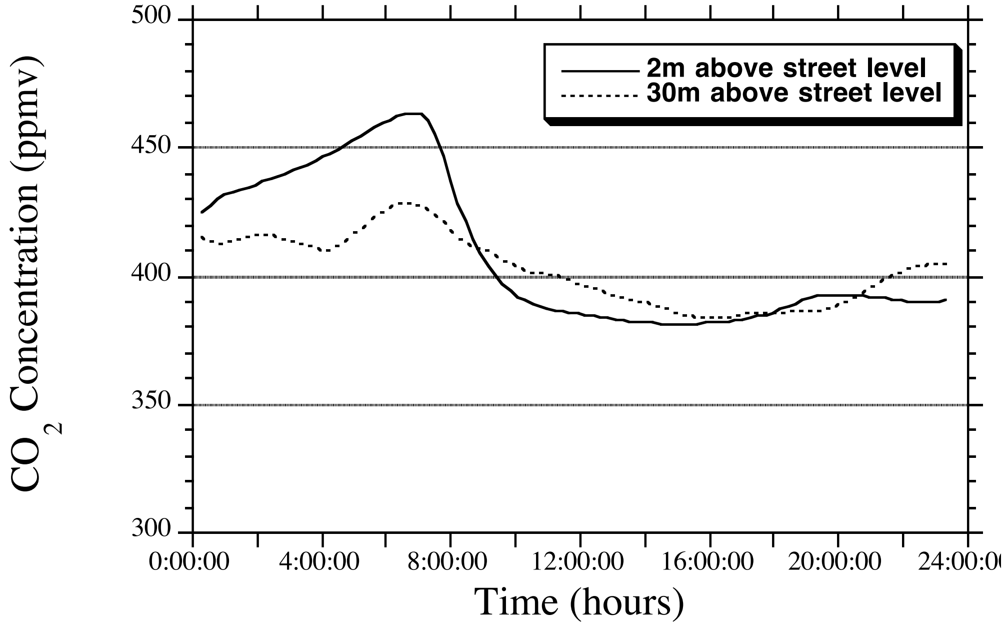

Figure 2. Hourly CO_2 Concentrations Recorded for a Typical Day in Brno (Stewart et al 2002).

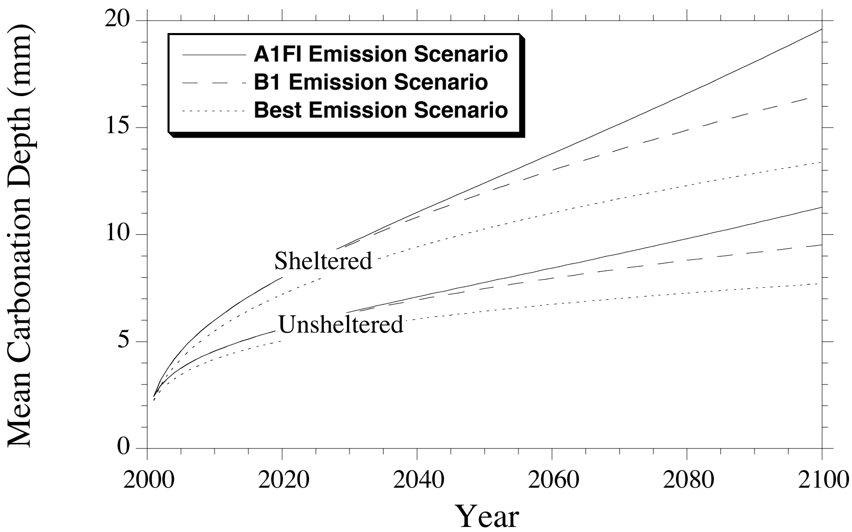

Figure 3. Mean Carbonation Depth for w/c=0.50 and Outdoor Sheltered and Unsheltered Exposures.

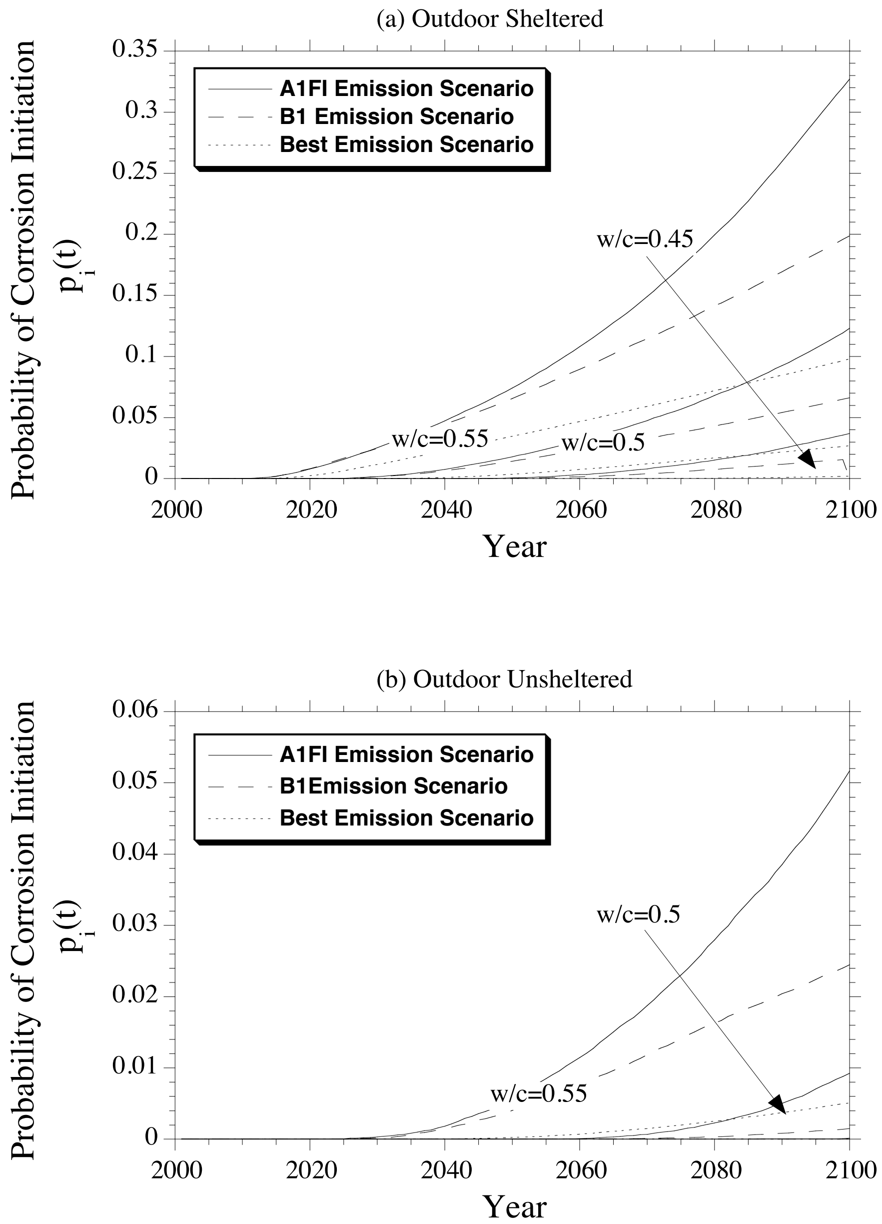

Figure 4. Probability of Corrosion Initiation for 30 mm Cover, for (a) Outdoor Sheltered and (b) Outdoor Unsheltered Exposures.

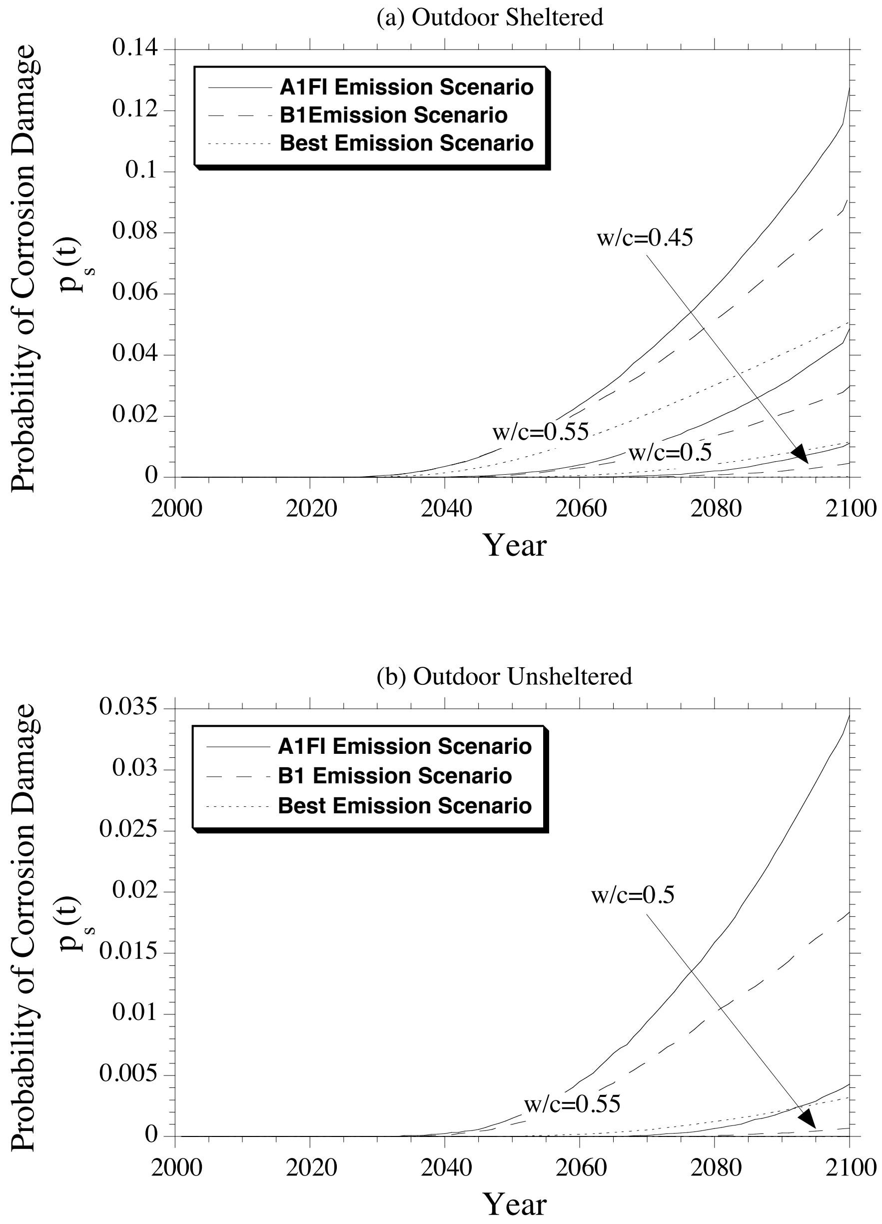

Figure 5. Probability of Corrosion Damage for 30 mm Cover, for (a) Outdoor Sheltered and (b) Outdoor Unsheltered Exposures.

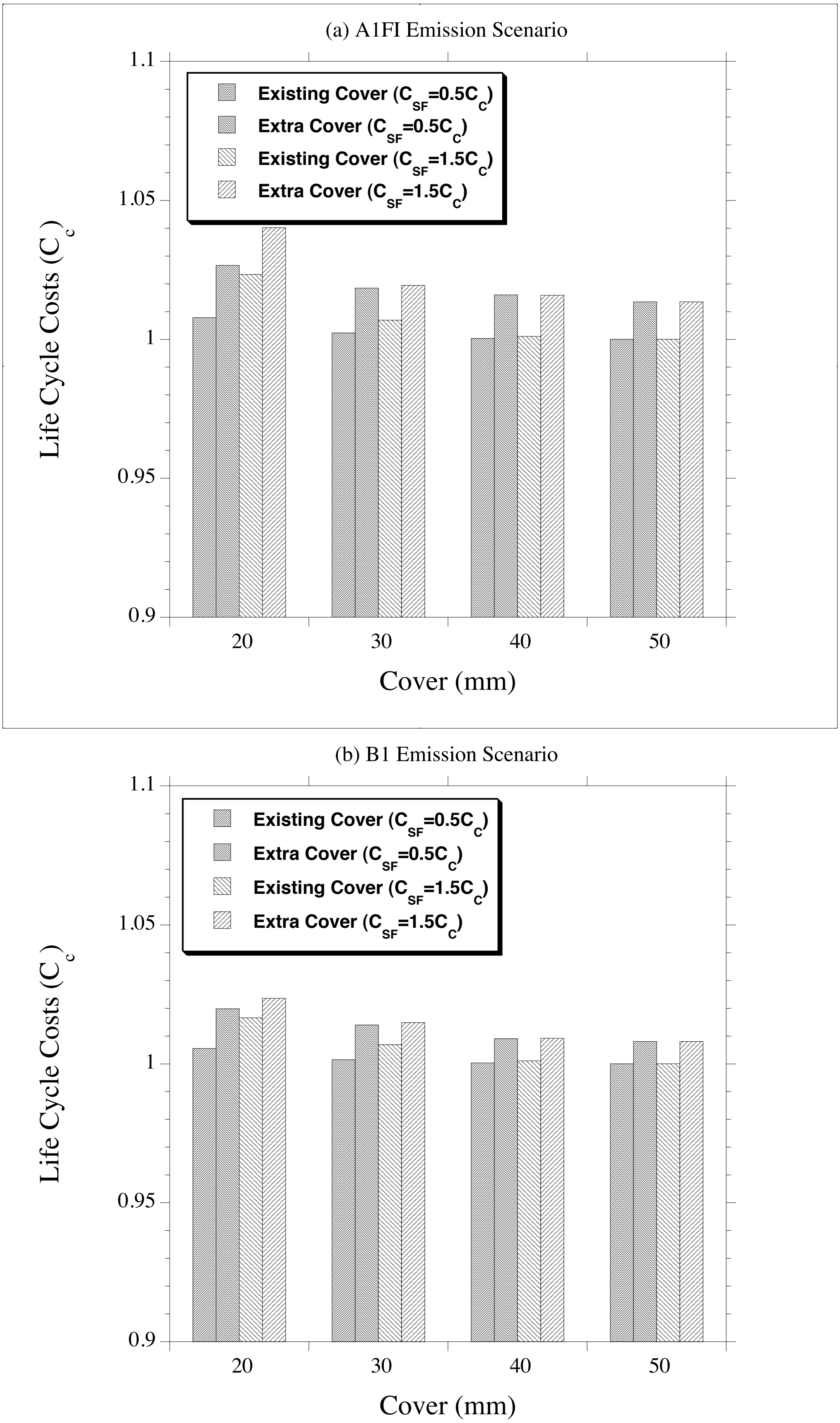

Figure 6. Life-Cycle Costs for w/c=0.5 and Y16 reinforcement, for (a) A1FI and (b) B1 Emission Scenarios.